CRYSTAL GROWTH OF ZNSE AND RELATED TERNARY COMPOUND SEMICONDUCTORS BY VAPOR TRANSPORT

Ching-Hua Su[1*], R. F. Brebrick[2], A. Burger[3], M. Dudley[4], N. Ramachandran[5]

NASA, Marshall Space Flight Center[1], Marquette University[2], Fisk University[3], State University of New York at Stony Brook[4], University Space Research Association[5]

1. Introduction

The objective of the project is to determine the relative contributions of gravity-driven fluid flows to the compositional distribution, incorporation of impurities and defects, and deviation from stoichiometry observed in the crystals grown by vapor transport as results of buoyance-driven convection and growth interface fluctuations caused by irregular fluid-flows. ZnSe and related ternary compounds, such as ZnSeS and ZnSeTe, were grown by vapor transport technique with real time in-situ non-invasive monitoring techniques. The grown crystals were characterized extensively to correlate the grown crystal properties with the growth conditions.

2. Previous Accomplishments

The following is the research progress in the past two years. In-situ monitoring of partial pressure by optical absorption technique and visual observation of the growing crystal were performed during vapor growth of ZnSe [1]. Low-temperature photoluminescence (PL) spectra and glow discharge mass spectroscopy (GDMS) were measured on ZnSe starting materials provided by various vendors and on bulk crystals grown from these starting materials by physical vapor transport (PVT) to study the effects of purification and contamination during crystal growth process [2]. Optical characterization was performed on wafers sliced from the grown crystals of ZnSe, ZnTe and $ZnSe_{1-x}Te_x$ (0<x<0.4). Energy band gaps at room temperature were determined from optical transmission measurements and a best fit curve to the band gap vs. composition, x, data gives a bowing parameter of 1.45 [3]. Low-temperature photoluminescence (PL) spectra of ZnSe and ZnTe were dominated by near band edge emissions and no deep donor-acceptor pairs were observed. The PL spectrum exhibited a broad emission for the $ZnSe_{1-x}Te_x$ samples, 0.09<x<0.39. The single broad PL emission spectra and the spectra measured as a function of temperature were interpreted as being associated with the exciton bound to Te clusters because of the high Te content in these samples [3].

3. Recent Results

a) *Beer Law constants and vapor pressures of HgI_2 over $HgI_2(s,l)$*

To validate numerical codes, in-situ monitoring during the PVT of HgI_2 was designed. The α-HgI_2 starting material was vacuum sublimated four times before zone refining in a zone refiner that produced a 1-in. melting zone. Fused silica tubing of 13 mm O. D., 10 mm I. D., and 60 cm in length was used as the zone-refining ampoule. The ampoule was first cleaned with an acetic-nitric-hydrofluoric acid solution, rinsed with de-ionized water and out-gassed under 10^{-3} Torr vacuum for 2 h. Then α-HgI_2 starting materials with a typical weight of about 100 g were loaded into ampoules. A total of 100 vertical zone passes with a zone travel rate of 8.5 cm/h were used. After the completion of the zone-refining process, the ampoules were

*Corresponding author. E-mail: ching.hua.su@msfc.nasa.gov

opened to recover the refined materials. The sample from the middle section (purest) was extracted and ground into powder.

The T-shaped optical cells were made of fused silica. The top of the T-shaped cell consisted of a 18 mm O.D., 15 mm I.D., cylindrical tube with flat, parallel windows and an optical path of about 10 cm. The bottom of the T-cell was a sidearm attached to the midpoint of the cell-proper. Two cells were made; HgI_2-1 was used to measure the optical absorption of HgI_2 sample as a function of temperatures and the other cell, HgI_2-2, was designed to measure Beer's Law constants by completely vaporizing the sample inside. For the HgI_2-1 cell, the sidearm was made by joining a 6 cm long, 12 mm O.D., 8 mm I.D. tube and a 10 cm long 18 mm O.D., 15 mm I.D. tube coaxially. The sidearm for the HgI_2-2 cell was made by joining a 2.5 cm long, 12 mm O.D., 8 mm I.D. tube and a 20 cm long 32 mm O. D., 28 mm I.D. tube. The 12 mm O.D. part was attached to the cell-proper and referred to as the stem and the larger O.D. part of the sidearm is referred as the reservoir section. For both cells, a 12 mm O. D., 8 mm I.D. tube was attached to the reservoir section for vacuum connection during seal-off. The volumes of the empty cells were measured as a function of the length along the sidearm by adding distilled water with 0.1 ml resolution. The empty cells were successively rinsed with distilled H_2O, 49 wt. % HF, distilled H_2O, methanol, distilled H_2O, acetone, and distilled H_2O and then dried in a box furnace at about 130°C. The cells were baked at about 850°C for 18 h under vacuum.

For the HgI_2-1 cell, 4.5765 g sample was weighed out using a Mettler AT 201 balance and loaded directly into the baked-out ampoule. For the complete vaporization cell, HgI_2-2, two small specks of HgI_2 were first loaded into a cleaned and baked quartz well (6 mm O. D., 4 mm I. D. and 2 cm long) to prevent any sample loss from sticking to the tubing wall during loading. The sample weighed 12.128 mg as determined with a Chyo Jupiter M1-20 microbalance, which was calibrated to an accuracy tolerance of 0.005 mg. The well was then slid into the optical proper region of the HgI_2-2 cell to minimize the loss from vaporization during seal-off. Both cells were sealed off at 1×10^{-4} Torr vacuum after 30 min of evacuation. The free volume of the cells were then determined from the sealed positions and were 36.2 ml and 138.0 ml, respectively, for HgI_2-1 and -2.

The sealed cells were placed in a five-zone T-shaped furnace. The top of the T was approximately 30 cm long and 4 cm I.D. and had three independently controlled heating zones. The two zones on the side (zone 1 and 3) consisted of two 7.5 cm long semi-cylindrical heating elements connected in parallel, and the central zone (zone 2) had one 7.5 cm long semi-cylindrical element. A ceramic tube liner, 28 cm long, (not shown in Figure 1) is positioned between the furnace bore and the optical cell-proper to block any stray light. The stem and the reservoir sections were heated, respectively, by a 4 cm I.D., 7.5 cm long and a 6.5 cm I.D., 30 cm long cylindrical element. A 45 cm long, 4 cm I.D., 6 cm O.D. heat pipe furnace liner (Dynatherm Corp.), with Hg working fluid inside, was inserted between the furnace bore and cell reservoir section to improve sample isothermality. Three K-type thermocouples, calibrated with standards and instrumentation traceable to N.I.S.T, were positioned along the optical cell-proper and three more along the stem and the sample section to check the temperature uniformity along the sample.

The furnace with the optical cell inside was then placed in the path of the sample beam of a double-beam, reversed-optics spectrophotometer (OLIS Inc., model 14H) with the reference beam passed under the furnace. The optical density, defined as $D = \log_{10}(I_{reference}/I_{sample})$, where I is the intensity (of reference or sample beams), was measured between the wavelength of 200 and 600 nm. The light source was a

598

deuterium lamp for wavelengths below 288 nm and a Xenon lamp for wavelengths above 288 nm. The typical instrument band pass was 0.16, 1.1, and 2.7nm, respectively at the wavelengths of 600, 288, and 200 nm. The temperature of the optical cell-proper, $T_{O.C.}$, was kept at 230, 260, 300 or 340 $\pm$ 1°C, while the stem and the reservoir sections were maintained at a temperature that was the same as or lower than $T_{O.C.}$. A baseline spectrum was measured first for each $T_{O.C.}$ with the reservoir temperature below 50°C.

For the HgI_2-1 cell, the optical density was measured with $T_{O.C.}$ at either 230 or 340°C, while the reservoir maintaining at a temperature lower than $T_{O.C.}$. A series of spectra were then measured for increasing reservoir/sample temperatures with times at fixed sample temperature generally about 20 min. For the HgI_2-2 cell, the $T_{O.C.}$ was initially set at 230°C and the optical density was measured as reservoir temperature increased. Between the reservoir temperature at 188 and 210°C, the measured optical density at specific wavelengths stopped to increase as temperature increased - indicating a complete vaporization of the sample. Then, the optical density spectra were measured with the whole cell under isothermal condition at 230, 260, 300, and 340°C to establish the Beer's Law constants.

The measured optical density for the HgI_2-1 cell, plotted in Figure 1, shows a triple-peak spectrum between 200 and 400 nm wavelength region. Neither the atomic absorption for the Hg $6\ ^1S_0 - 6\ ^3P_1$ transition at 254 nm nor the vibronic absorption spectrum for I_2 molecule from 400 to 600 nm with a maximum at 505 nm were observed. The measured spectrum is consistent with the published absorption spectra for HgI_2 [9]. Since there was no absorption observed at the wavelength of 600 nm, the net optical density was obtained by subtracting the baseline from the measured spectrum with a correction of the baseline shift determined from the measured optical density at 600 nm. The measurable upper limit for D was 3.5 to 4, where the sample beam intensity reduced to the same order of magnitude as the dark current in the photomultiplier tube. The net optical density, D, for a set of wavelengths between 200 and 440 nm were plotted against 1000/T, where T is the reservoir temperature in K. For both $T_{O.C.}$ (230 and 340°C), the data for each wavelength are parallel, implying that the absorption in the range of these wavelength was from the same vapor species. For the HgI_2-2 cell, the plot of D vs. 1000/T clearly shows that the sample completely vaporized at 197 $\pm$ 1°C. The errors in the measured D and temperatures were estimated to be less than $\pm$ 0.001, and $\pm$ 1.0°C, respectively.

In the subsequent isothermal runs for the HgI_2-2 cell, the measured D were off-scale for all the wavelengths below 300 nm, except at 212 nm, and were too low to be reliable for wavelengths higher than 400 nm. The measured D for six wavelengths, i.e. 212 nm and 5 wavelengths between 300 to 380 nm, were used to determine Beer's Law constants, α. The pressure was calculated from ideal gas law, $P = nRT/V$, where n, R and V are, respectively, the number of mole, gas constant and the free volume. Table 1 gives the Beer's Law constants of HgI_2 species for these 6 wavelengths at four different temperatures, 230, 260, 300, and 340°C.

Using the Beer's Law constants given in Table 1, the vapor pressures of HgI_2 as a function of temperatures were determined from the measured D in the HgI_2-1 runs. The pressure value was taken as the average of, typically, 4 to 6 wavelengths and is plotted as a function of 1000/T in Figure 2. The measured pressures ranged from 9 x 10^{-6} to 0.8atm and the results from the optical cell temperatures at 340 and 230°C agree well. The data measured by Abraham et al. [4] in the temperature range of 417 and 509 K is given as the dotted line. Our data agree well with their data in the temperature range of 417 to 460 K and are a little higher in the high temperature region. The HgI_2 pressures measured by Piechotka et al. [5] were
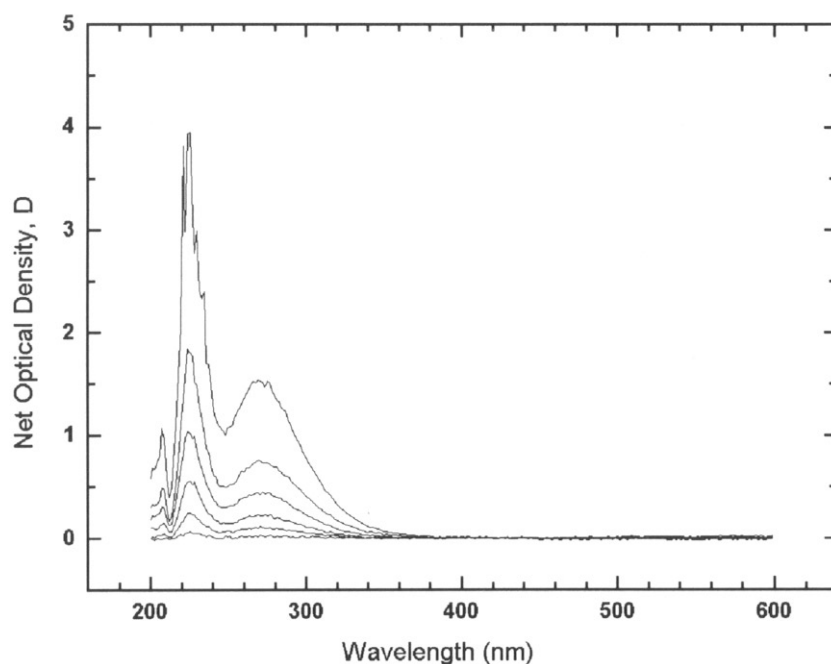
Figure 1. Optical absorption spectra of HgI_2 vapor species at six different reservoir temperatures from low to high absorption as 360, 386, 408.4, 419.8, 429.6, and 443.9K. ($T_{O.C.}$ = 340°C)

Table 1. Beer's Law constants, α, in atm-cm for HgI_2 vapor species.

Wavelength (nm)	α at 230 °C	α at 260 °C	α at 300 °C	α at 340 °C
212	0.0851	0.0831	0.0833	0.0799
300	0.0335	0.0352	0.0359	0.0379
320	0.0914	0.0894	0.0861	0.0855
342	0.3377	0.3101	0.2849	0.2739
360	1.0637	0.9739	0.8398	0.7420
380	3.6759	3.9883	2.7200	2.6388
208	0.0201*			0.0260*
224	0.00658*			0.00759*
230	0.00912*			0.00938*
242.5	0.0276*			0.0262*
265	0.0148*			0.0188*
280	0.0169*			0.0214*
400	2.1435*			7.6955*
420	4.0307*			23.680*
440	4.4392*			79.119*

* α determined from HgI_2 −1 runs

represented by three expressions for temperatures between 300 and 420 K. The expressions for the two high temperature sections are shown as the dashed line in Figure 4. In general, the agreement between our

600

data and their results are good. Omaly et al. [6] claimed to deduce from the JANAF thermodynamic data [7] the HgI_2 equilibrium pressures, which is shown as the lowest dashed-dotted line.
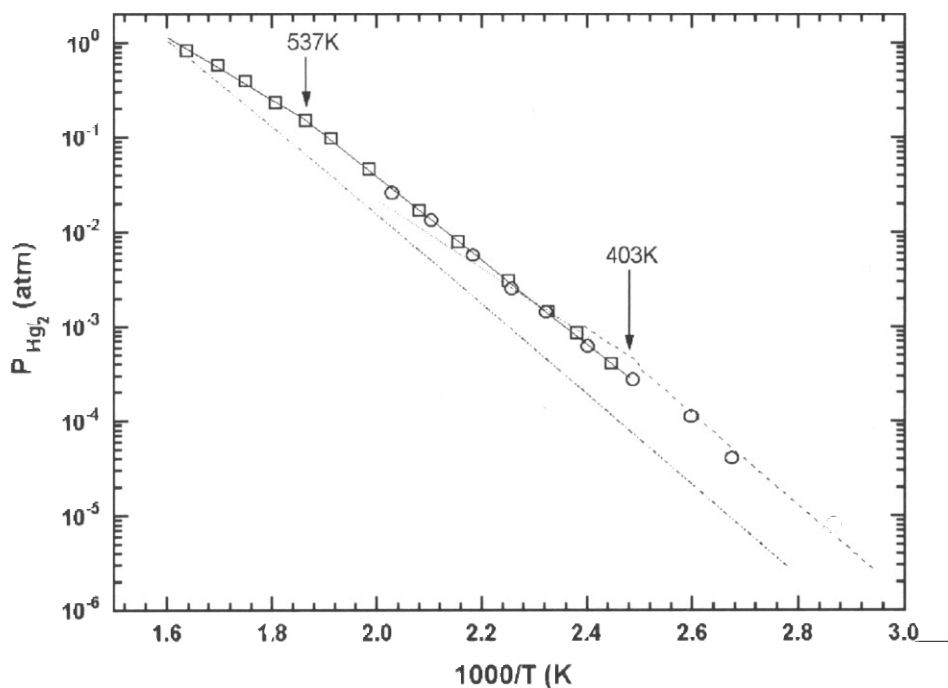
Figure 2. $\log_{10} P_{HgI2}$ vs. 1000/T, where T is reservoir temperature in K. Squares and circles are measured for $T_{O.C.}$ at 340 and 230°C, respectively. The two solid line segments are given by Eq. (1) and (2). The dashed line at low temperature region is from Ref. [5], and the dotted line in the middle temperature range is from Ref [4]. The lowest dashed-dotted line is from Ref [6].

The temperature for the α to β–HgI_2 transition as well as the melting point were studied by Differential Scanning Calorimetry [8] and were found to be dependent on the purity and stoichiometry of the sample. For the high purity sample, the α to β transition and the melting point were found to be 405 ± 2 K and 531 ± 1 K, respectively. Therefore, the vapor pressure data for T > 531 K and 405 < T < 531 K were fit linearly on the ln P vs. 1/T plot and the best fits are as follows:

$$\ln P \text{ (atm)} = -7,700/T + 12.462 \qquad\qquad T > 531 \text{ K} \qquad\qquad (1)$$
$$\ln P \text{ (atm)} = -10,150/T + 17.026 \qquad\qquad 405 < T < 531 \text{ K} \qquad (2)$$

The expressions correspond to the enthalpies of vaporization and sublimation of 15.30 and 20.17 Kcal/mole, respectively, for the liquid and the β–phase HgI_2, and the intersection of the two expressions gives a melting point of 537 K. The difference in the enthalpies gives an enthalpy of fusion of 4.87 Kcal/mole. The enthalpy of sublimation for β–HgI_2, 20.17 Kcal/mole, is in good agreement with previous results of 20.267 Kcal/mole [5] and 20.0 Kcal/mole [9] and is about 2 % higher than the value of 19.789 Kcal/mole given in Ref. [4]. The enthalpy of fusion agrees well with the value of 4.9 Kcal/mole [9] and about 8 % higher than the value of 4.5 Kcal/mole quoted in Ref. [7] and [10].

The Beer's Law constants for those wavelengths other than listed in Table 1 can be calculated from the P_{HgI_2} for each of the HgI_2–1 runs, the measured D for the specific wavelength, and the path length. The Beer's Law constants were then taken as the average of the calculated values from 4 to 6 runs at different

601

reservoir temperatures. Table 1 lists the Beer's Law constants for these wavelengths at the specific optical cell temperature, 230 or 340°C. Using these Beer's Law constants and the measured D, one can calculate the pressures for each of the HgI_2–1 runs and, as expected, they agree well with the data presented in Figure 4 except that a value for P_{HgI_2} at the lowest reservoir temperature, 349K, was obtained.

The extinction coefficients at 342 nm were determined [4] as a linear function of T:

$$\varepsilon \text{ (liter mole}^{-1} \text{ cm}^{-1}) = 0.803 \text{ T (K)} - 273.1 \qquad (3)$$

The Beer's Law constants, α, can be converted to the extinction coefficient using $\varepsilon = RT/\alpha$. The values for ε at 342 nm calculated from the values for α given in Table 1 were 122.237, 141.076, 165.065, and 183.711, respectively, for 230, 260, 300, and 340 °C. The values given by Eq. (3) are 7, 10, 13, and 19 % higher than our data at 260, 260, 300, and 340°C, respectively.

There were three P_{HgI_2} data below 405 K for the solid α–phase, and they show a similar slope in the log P vs. 1/T plot as that for the β–phase. The enthalpy of sublimation for α–HgI_2 was not determined because there were not enough data points and also because, in the 10^{-6} to 10^{-4}atm range, the associated errors in the measured P were relatively large. Since the reported enthalpy of transition from α to β–HgI_2 was small, about 640 cal/mole [10], the slope of the log P vs. 1/T plot for the α–phase should be very close to that for the β–phase. The enthalpy of vaporization for the liquid phase was determined from five data points and, therefore, the error was larger than the enthalpy of sublimation for the β–phase, which was determined from 15 data points. Consequently, the heat of fusion and the melting point, which were derived from the two expressions in Eq. (1) and (2), will inherit the error for the liquid phase. However, it should be noted that the errors associated with the Beer's Law constants only affect the absolute values of the measured pressures, but not the slope in the log P vs. 1/T plot.

b) *Partial Pressures for Several In-Se Compositions from Optical Absorbance of the Vapor*

The optical absorbance of the vapor phase over various In-Se compositions between 33.3 and 60.99 at% and 673 to 1418 K has been measured and used to obtain the partial pressures of $Se_2(g)$ and $In_2Se(g)$ [11]. The results are in agreement with silica Bourdon gage measurements for compositions between 50 and 61 atomic % but significantly higher than those from Knudsen cell and simultaneous Torsion-Knudsen cell measurements. It is found that 60.99 at% Se lies outside the sesquiselenide homogeneity range and 59.98 at% Se lies inside and is the congruently melting composition. The Gibbs energy of formation of the liquid from its pure liquid elements between 1000 and 1300 K is essentially independent of temperature and falls between -36 and -38 kJ per gram atomic weight for 50 and 56 % Se at 1200 and 1300 K.

References

1. Ching-Hua Su, S. Feth and S. L. Lehoczky, J. Crystal Growth 209 687-694 (2000).
2. Ching-Hua Su, S. Feth, Ling Jun Wang and S. L. Lehoczky, J. Crystal Growth 224 32-40 (2001).
3. Ching-Hua Su, S. Feth, Shen Zhu, S. L. Lehoczky and Ling Jun Wang, J. Appl. Phys. 88 5148-5152 (2000).
4. B. M. Abraham and A. Jeannotte, Inorg. Chem., 16 (1977) 2270.
5. M. Piechotka and E. Kaldis, J. Less-Common Metals, 115 (1986) 315.
6. J. Omaly, M. Robert, P. Brisson and R. Cadoret, Nucl. Instr. Meth. 213 (1983) 19.
7. JANAF International Table, 2nd Ed. (1971).

8. K.-T. Chen, L. Salary, A. Burger, E. Soria, A. Antolak and R. B. James, Nucl. Instr. Meth. Phys. Res. A 380 (1996) 53.
9. J. Rinse, Rec. Trav. Chim., 47 (1928) 33.
10. R. Rolsten, Iodide Metals and Metal Iodides, John Wiley & sons, Inc. (1961).
11. R. F. Brebrick and Ching-Hua Su, to be published on J. Phase Equilibria (2002).